N-Methyltryptophan Oxidase from *Escherichia coli*: Reaction Kinetics with *N*-Methyl Amino Acid and Carbinolamine Substrates[†]

Peeyush Khanna and Marilyn Schuman Jorns*

Department of Biochemistry, MCP Hahnemann School of Medicine, Philadelphia, Pennsylvania 19129

Received October 20, 2000

ABSTRACT: *N*-Methyltryptophan oxidase (MTOX), a flavoenzyme from *Escherichia coli*, catalyzes the oxidative demethylation of *N*-methyl-L-tryptophan (k_{cat} = 4600 min^{-1}). Other secondary amino acids (e.g., sarcosine) are oxidized at a slower rate. We have identified carbinolamines as a new class of alternate substrate. MTOX oxidation of the carbinolamine formed with L-tryptophan and formaldehyde yields *N*-formyl-L-tryptophan in a relatively slow reaction that does not compete with turnover of MTOX with *N*-methyl-L-tryptophan. Double reciprocal plots with *N*-methyl-L-tryptophan as the varied substrate are nearly parallel, but the slopes show a small, systematic variation depending on the oxygen concentration. *N*-Benzylglycine, a dead-end competitive inhibitor with respect to *N*-methyl-L-tryptophan, acts as a noncompetitive inhibitor with respect to oxygen. The results are consistent with a modified ping pong mechanism where oxygen binds to the reduced enzyme prior to dissociation of the imino acid product. MTOX is converted to a 2-electron reduced form upon anaerobic reaction with *N*-methyl-L-tryptophan, sarcosine, or the carbinolamine formed with L-tryptophan and formaldehyde. No evidence for a detectable intermediate was obtained by monitoring the spectral course of the latter two reactions. MTOX reduction with thioglycolate does, however, proceed via a readily detectable anionic, flavin radical intermediate. The reductive half-reaction with sarcosine at 4 °C exhibits saturation kinetics (k_{lim} = 6.8 min^{-1}, K = 39 mM) and other features consistent with a mechanism in which a nearly irreversible reduction step (E_{ox}•S → E_{red}•P) (k_{lim}) is preceded by a rapidly attained equilibrium (K) between free E and the E•S complex. The 21 °C temperature difference can reasonably account for the 3.6-fold lower value obtained for k_{lim} as compared with turnover at 25 °C (k_{cat} = 24.5 min^{-1}), suggesting that sarcosine is oxidized at a kinetically significant rate under anaerobic conditions and the reductive half-reaction is rate-limiting during turnover. These conclusions are, however, difficult to reconcile with steady-state kinetic patterns obtained with sarcosine that are consistent with a rapid equilibrium ordered mechanism with oxygen as the *first* substrate. The basis for the apparent stability of the MTOX•oxygen complex (K_d = 72 μM) is unknown.

N-Methyltryptophan oxidase (MTOX)[1] is a newly discovered monomeric flavoenzyme (42 kDa) from *Escherichia coli* that contains covalently bound FAD [8α-(*S*-cysteinyl)FAD] (*1*). MTOX preferentially catalyzes the oxidative demethylation of *N*-methyl-L-tryptophan but will also oxidize other *N*-methyl amino acids. Although the gene encoding MTOX (*solA*) was isolated based on strong sequence homology (43% amino acid identity) with monomeric sarcosine oxidase (MSOX) (*2*), sarcosine is a poor substrate for MTOX. MTOX is expressed as a constitutive enzyme in a wild-type *E. coli* K-12 strain (*3*). Expression is enhanced by growth on minimal media but not induced by *N*-methyltryptophan, unlike MSOX expression which is induced by growth on sarcosine, a common soil metabolite that can provide a source of carbon and energy for various bacteria (*4*). The metabolic role and distribution of other *N*-methyl amino acids is not well-characterized although *N*-methyltryptophan has been identified in certain plant species and *N*-methyl amino acids are found in polyketide antibiotics (*5*, *6*). The physiological role of MTOX in *E. coli* in unknown. The active site of MTOX has been probed by characterization of the properties and reactivity of its prosthetic group and by the identification of various active site ligands (*3*). MTOX is a member of a recently recognized family of prokaryotic and eukaryotic amine oxidases that all contain covalently bound flavin. Other family members include MSOX, pipecolate oxidase, and heterotetrameric sarcosine oxidase (*1*, *7*, *8*). The crystal structures of free MSOX and various inhibitor complexes have recently been determined (*9*, *10*).

In this paper, the mechanism of MTOX catalysis has been investigated in steady state and reductive-half reaction studies with *N*-methyl-L-tryptophan, sarcosine, and a thiolate substrate analogue. We also report the identification of carbinolamines as a new class of alternate substrate for MTOX and kinetic evidence for an MTOX•oxygen complex.

EXPERIMENTAL PROCEDURES

Materials. Horseradish peroxidase, glucose oxidase (*Aspergillus niger*, Type V-S) *o*-dianisidine, methyl viologen,

[†] This work was supported in part by Grant GM 31704 from the National Institutes of Health.

* To whom correspondence should be addressed. Phone: (215) 991-8580. FAX: (215) 843-8849. E-mail: marilyn.jorns@drexel.edu.

[1] Abbreviations: MTOX, *N*-methyltryptophan oxidase; MSOX, monomeric sarcosine oxidase; FAD, flavin adenine dinucleotide; EDTA, ethylenediaminetetraacetic acid; FAD•−, anionic FAD radical; FADH−, 1,5-dihydroFAD anion.

10.1021/bi002442t CCC: $20.00
Published on Web 01/11/2001

thioglycolic acid, *N*-methyl-L-tryptophan, L-tryptophan, *N*-formyl-DL-tryptophan, and L-proline were purchased from Sigma. Sarcosine and *N*-benzylglycine were obtained from Aldrich. Formaldehyde was from Fisher. Precoated thin-layer chromatography plates (silica gel 60, F-254) were from E. Merck.

Enzyme Purification and Assay. Purification of recombinant MTOX from *Escherichia coli* and MSOX from *Bacillus sp. B-0618*, routine protein and activity assays were performed as described by Wagner et al. (*1*). The concentration of MTOX was estimated using the previously determined extinction coefficient ($\in_{457} = 13\ 300\ M^{-1}\ cm^{-1}$, pH 8.0) (*1*).

Spectroscopy. Absorption spectra were recorded using a Perkin-Elmer Lambda 2S spectrometer. Spectral titrations with active site ligands were conducted at 4 °C in 50 mM potassium phosphate buffer, pH 8.0, containing 1 mM EDTA. For comparison with spectral perturbations observed with other ligands, titration data obtained with *N*-formyl-DL-tryptophan were normalized to the same initial concentration of uncomplexed MTOX ($A_{457} = 0.5$, 37.6 μM MTOX); the difference spectrum for 100% complex formation was calculated, as previously described (*3*).

Anaerobic experiments were conducted using a special cuvette, as previously described (*10*). Unless otherwise noted, reaction mixtures contained an oxygen-scavenging system consisting of glucose oxidase, glucose, and catalase, similar to that previously described (*11*). This system was omitted in reactions involving formaldehyde and L-tryptophan (or glycine) as reductant.

Steady-State Kinetics. Studies were conducted at 25 °C by monitoring hydrogen peroxide formation using a horseradish peroxidase coupled assay. Formation of oxidized *o*-dianisidine was monitored by the increase in absorbance at 460 nm ($\in_{460} = 6765\ M^{-1}\ cm^{-1}$). Reactions were performed in 100 mM potassium phosphate buffer, pH 8.0, containing 1 mM EDTA, amino acid, oxygen, and inhibitor, as indicated, 320 μM *o*-dianisidine, and 2.4 U horseradish peroxidase in a total volume of 350 μL. Assays were initiated by addition of MTOX.

A standard semimicro cuvette was used for reactions in air-saturated buffer. A special cuvette (Spectrocell) with a screw-cap equipped with a Teflon-silicone membrane was used in studies where the oxygen concentration was varied. Reaction mixtures containing all components except horseradish peroxidase and MTOX were equilibrated by bubbling at 25 °C for 30 min with gas mixtures containing 5.0, 10.2, 21, 44, or 100% oxygen (balance nitrogen), similar to that previously described (*11*). Horseradish peroxidase (6.5 μL) was injected, and the cuvette was placed into a thermostated cell holder of a Perkin-Elmer λ2S spectrophotometer for a 3-min incubation at 25 °C. Reactions were initiated by injecting a 5 μL aliquot of MTOX. Oxygen concentrations were calculated based on the dissolved oxygen concentration obtained after equilibration with 100% oxygen (1.3 mM) (*12*) and were corrected for the 11.5 μL addition of enzymes in air-saturated buffer.

Thin Layer Chromatography. Samples were spotted on fluorescent indicator, silica gel plates. Tryptophan derivatives were visualized as dark spots under ultraviolet light. Chromatograms were developed using chloroform/methanol/formic acid, 85:13:2 (solvent A) or ethyl acetate/formic acid, 80:20 (solvent B). L-Tryptophan and *N*-formyl-L-tryptophan were separated using solvent A ($R_f = 0$ and 0.19, respectively). L-Tryptophan, *N*-formyl-L-tryptophan, and *N*-methyl-L-tryptophan were separated using solvent B ($R_f = 0.73$, 0.88, and 0.66, respectively). Reactions initiated by mixing MTOX with formaldehyde and L-tryptophan were microfiltered (Microcon-10) after a 5.3 h incubation at room temperature. The filtrate was analyzed using solvent A. In the case of reactions initiated by mixing MTOX with *N*-methyl-L-tryptophan, aliquots were withdrawn after various periods of incubation at room temperature, heated for 5 min at 100 °C to denature MTOX, and then microfiltered. The filtrates were analyzed using solvent B.

Data Analysis. Data were fit to eqs 1−7 using the curve fit function in Sigma Plot (Jandel Corporation). Equation 1 was used for (i) analysis of the apparent first-order rate of enzyme reduction by sarcosine (k_{obs}) as a function of the substrate concentration. *Y* and *A* are k_{obs} and k_{lim}, respectively. *X* is the sarcosine concentration, and *K* is the apparent dissociation constant of the E·S complex. (ii) Analysis of titration data with *N*-formyl-DL-tryptophan and thioglycolate. *Y* and *A* are the observed and maximal absorbance change at the wavelength selected for analysis, respectively, *X* is the concentration of the varied ligand and *K* is the complex dissociation constant. Equation 2 was used to fit the apparent first-order kinetics observed for the reduction of MTOX with sarcosine or formaldehyde plus L-tryptophan ($k_{obs} = k$). *Y* is the observed absorbance at the selected wavelength and time = *t*, *A* is the maximal absorbance change, and *B* is the final absorbance at the selected wavelength. Equation 3 was used to fit the biphasic kinetics of the anaerobic reduction of MTOX with thioglycolate. *Y* is the observed absorbance at the selected wavelength and time = *t*, *A* and *B* are the maximal absorbance changes in the first and second phases of the reaction, *k* and *j* are the corresponding rate constants, and *C* is the final absorbance at the selected wavelength.

$$Y = \frac{AX}{X + K} \tag{1}$$

$$Y = Ae^{-kt} + B \tag{2}$$

$$Y = Ae^{-kt} + Be^{-jt} + C \tag{3}$$

$$v = \frac{V_{max}AB}{K_{ia}K_b + K_aB + K_bA + AB} \tag{4}$$

$$v = \frac{V_{max}AB}{(1 + I/K_i)(K_{ia}K_b + K_aB) + K_bA + AB} \tag{5}$$

$$v = \frac{V_{max}AB}{K_aK_b + K_bA + AB} \tag{6}$$

Equation 4 was used to fit the steady-state kinetic data obtained at various concentrations of *N*-methyl-L-tryptophan and oxygen. K_a and K_b are the K_m values for amino acid and oxygen, respectively. K_{ia} is the inhibition constant for the amino acid. Steady-state kinetic data obtained at a fixed *N*-methyl-L-tryptophan concentration and various concentrations of oxygen and *N*-benzylglycine were fit to eq 5 using values determined for K_a, K_b, and K_{ia} in the absence of inhibitor. K_i is the dissociation constant for the MTOX•*N*-benzylglycine complex and *I* is inhibitor concentration.

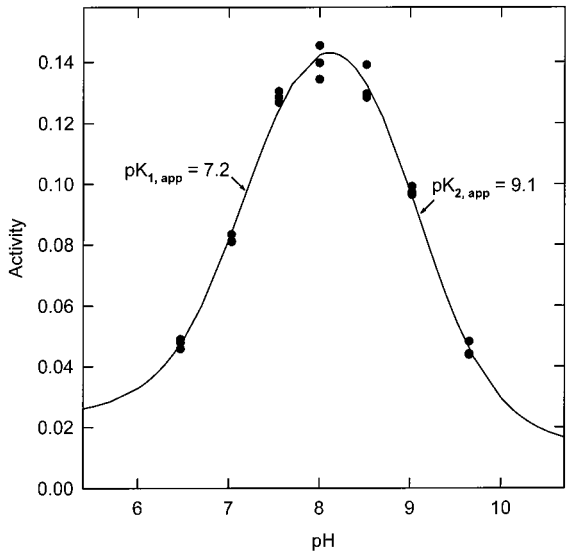

FIGURE 1: pH activity profile. MTOX activity was measured at 25 °C in air-saturated potassium phosphate buffer (50 mM) containing 1 mM *N*-methyl-L-tryptophan in a coupled assay using horseradish peroxidase (*1*). The solid line shows the fit of the data to eq 7.

Equation 6 was used to fit the steady-state kinetic data obtained at various concentrations of sarcosine and oxygen. K_a and K_b are the dissociation constants of oxygen and sarcosine from the MTOX•oxygen and MTOX•oxygen• sarcosine complexes, respectively. Equation 7 is described in Results.

RESULTS

pH Activity Profile. MTOX activity was measured as a function of pH and found to exhibit a bell-shaped pH-activity curve with an optimum at pH 8 (Figure 1). The data could be fitted to a double ionization titration curve (eq 7) (*13*) where $A_{EH_2^+}$, A_{EH}, or A_{E^-} is the activity due to the corresponding enzyme form (EH_2^+, EH or E^-, respectively) and K_1 and K_2 are the indicated dissociation constants. The

$$A_{obs} = \frac{[H^+]^2 A_{EH_2^+} + [H^+]K_1 A_{EH} + K_1 K_2 A_{E^-}}{K_1 K_2 + [H^+]K_1 + [H^+]^2}$$

$$EH_2^+ \overset{K_1}{\rightleftharpoons} EH + H^+$$

$$EH \overset{K_2}{\rightleftharpoons} E^- + H^+$$

analysis indicates that maximal activity is observed with EH, a form where a group with an apparent pK_a of 7.2 is unprotonated and a group with an apparent pK_a of 9.1 is protonated. On the basis of these results, pH 8.0, was selected as the pH for steady state and reductive half-reaction studies.

Steady-State Kinetics with N-Methyl-L-tryptophan. Double-reciprocal plots of reaction rate versus *N*-methyl-L-tryptophan concentration at various oxygen concentrations are linear and almost parallel (Figure 2). The slopes, however, show a small but systematic variation depending on the oxygen concentration, as judged by linear regression analysis. This suggests that turnover of MTOX with *N*-methyl-L-tryptophan does not proceed via a classic ping pong mechanism where the first product dissociates prior to reaction of oxygen with the

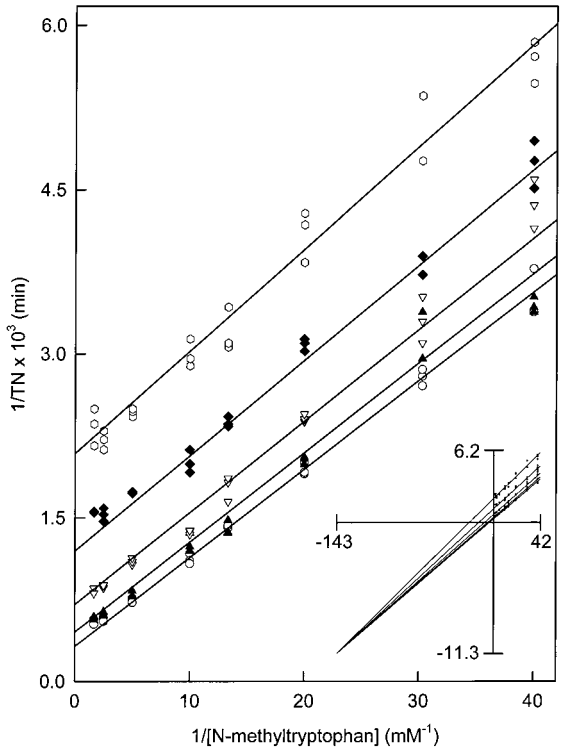

FIGURE 2: Steady-state kinetic data for MTOX with *N*-methyl-L-tryptophan as substrate. Measurements were made at 25 °C in 100 mM potassium phosphate buffer, pH 8.0, at various oxygen concentrations [1.27 mM (open circles), 0.56 mM (filled triangles), 0.27 mM (open triangles), 0.14 mM (filled diamonds), 0.072 mM (open hexagons)]. The lines represent the fit of the data to eq 4. The convergence of the fitted lines is illustrated in the inset where the data have been replotted according to a different scale.

reduced enzyme. The data are consistent with a modified ping pong mechanism where oxygen reacts with the reduced enzyme prior to the release of the first product (Scheme 1). Steady-state kinetic parameters, obtained by fitting the data to the rate equation for a modified ping pong mechanism (eq 4), are similar to those estimated by linear regression analysis (Table 1).

Inhibition by N-Benzylglycine. N-Benzylglycine binds to the active site of MTOX, perturbs the flavin absorption spectrum, and acts as a dead-end competitive inhibitor with respect to *N*-methyl-L-tryptophan (*3*). *N*-Benzylglycine should exhibit noncompetitive inhibition with respect to oxygen in the case of a modified ping pong mechanism whereas uncompetitive inhibition is predicted for a classic ping pong mechanism (*14*). Double-reciprocal plots of velocity versus oxygen concentration at different concentrations of *N*-benzylglycine and a fixed concentration of *N*-methyl-L-tryptophan are linear. The slopes and intercepts varied depending on the inhibitor concentration, as indicated by linear regression analysis (Figure 3). A value for the inhibition constant ($K_i = 7.40 \pm 0.5$ mM) was obtained by fitting the data to an equation for a modified ping pong mechanism in the presence of a dead-end inhibitor that combines only with E (eq 5). The observed K_i value is in good agreement with the K_d value obtained for *N*-benzylglycine complex with MTOX by spectral titration under the same reaction conditions ($K_d = 8.7$ mM) (*3*). The results provide further evidence that turnover of MTOX with *N*-methyl-L-tryptophan occurs via a modified ping pong mechanism.

Scheme 1: Modified Ping Pong Mechanism

$$E_{ox} \underset{k_{-1}}{\overset{k_1[S]}{\rightleftharpoons}} E_{ox}{\cdot}S \underset{k_{-2}}{\overset{k_2}{\rightleftharpoons}} E_{red}{\cdot}P \underset{k_{-3}}{\overset{k_3[O_2]}{\rightleftharpoons}} E_{red}{\cdot}P{\cdot}O_2 \underset{k_{-4}}{\overset{k_4}{\rightleftharpoons}} E_{ox}{\cdot}P{\cdot}Q \underset{k_{-5}}{\overset{k_5}{\rightleftharpoons}} E_{ox}$$

Table 1: Steady-State Kinetic Parameters with *N*-Methyl-L-tryptophan as Substrate[a]

parameter	
k_{cat} (min^{-1})	4600 ± 900 (4600)
$K_{m\ amino\ acid}$ (mM)	0.37 ± 0.08 (0.37)
$K_{m\ oxygen}$ (mM)	0.61 ± 0.1 (0.61)
$K_{ia\ amino\ acid}$ (μM)	7.0 ± 2 (6.8)

[a] Parameters were determined by fitting the data to an equation for a modified ping pong mechanism (eq 4). The values shown in parentheses were determined by linear regression analysis of double reciprocal plots, as described in the text.

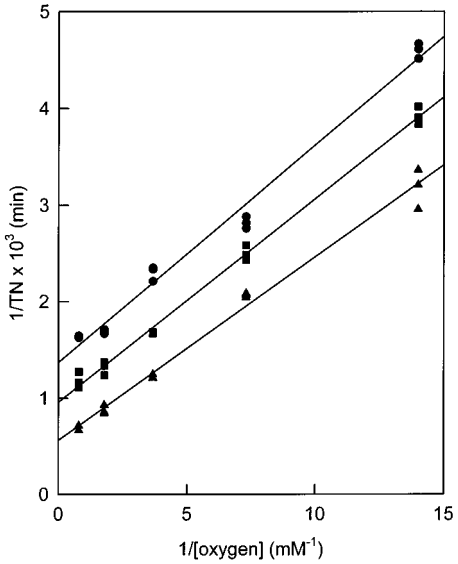

FIGURE 3: *N*-benzylglycine inhibition with respect to oxygen. Measurements were made at 1.0 mM *N*-methyl-L-tryptophan and the following inhibitor concentrations: 0 mM (solid triangles), 25 mM (solid squares), and 50 mM (solid circles). The lines show a linear regression analysis of the data.

Reduction of MTOX with N-Methyl-L-tryptophan or Sarcosine. Anaerobic reaction of MTOX with 0.2 mM *N*-methyl-L-tryptophan results in the immediate conversion to 1,5-dihydroFAD, as judged by the characteristic bleaching of the oxidized flavin spectrum (Figure 4, panel A, inset). The entire spectral course of the anaerobic half-reaction can be monitored in a simple manual mixing experiment by replacing *N*-methyl-L-tryptophan with the same concentration of sarcosine, a poor substrate for MTOX. An isosbestic conversion of oxidized enzyme to 1,5-dihydroFAD is observed upon reaction with sarcosine (Figure 4, panel A). The results provide no evidence for a spectrally detectable intermediate in the reductive half-reaction.

Reductive Half-reaction and Steady-State Kinetics with Sarcosine. The reductive half-reaction at higher concentrations of sarcosine was too fast to monitor in a manual mixing experiment at 25 °C but could be measured at 4 °C. Apparent first-order kinetics were observed over a wide range of

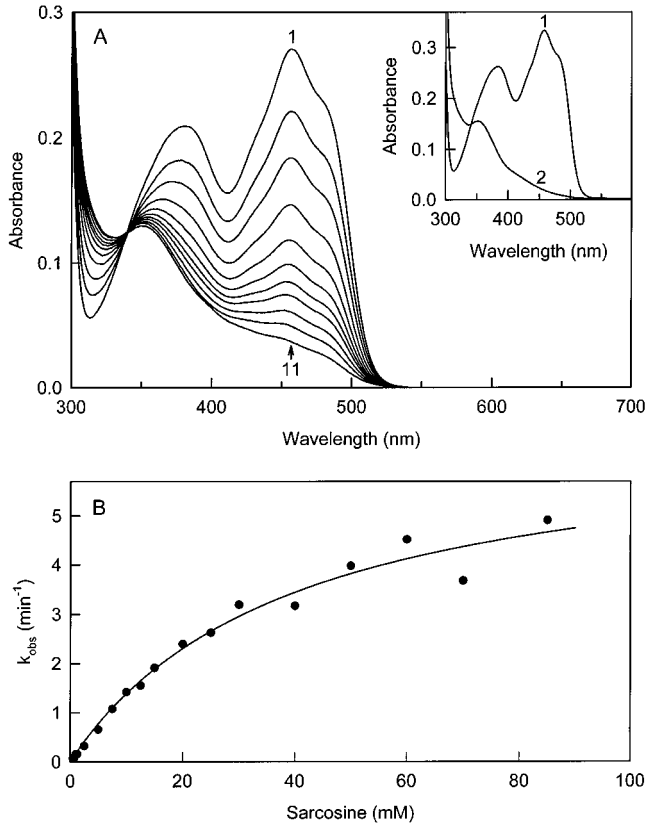

FIGURE 4: Reduction of MTOX with *N*-methyl-L-tryptophan or sarcosine. Reactions were conducted under anaerobic conditions in 50 mM potassium phosphate buffer, pH 8.0, containing 1 mM EDTA at 25 °C (panel A) or 4 °C (panel B). Panel A: Curves 1−11 were recorded 0, 1, 5, 10, 15, 20, 25, 30, 40, 60, and 960 min, respectively, after adding 0.2 mM sarcosine. Curves 1 and 2 in the inset show spectra before and immediately after mixing with 0.2 mM *N*-methyl-L-tryptophan. Panel B: The observed rate of the anaerobic half-reaction with sarcosine is plotted as a function of the substrate concentration. The solid line is a fit of the data to a hyperbolic saturation curve (eq 1).

sarcosine concentrations (0.5 to 85 mM). A plot of k_{obs} versus sarcosine concentration was hyperbolic (Figure 4, panel B) ($k_{lim} = 6.8 \pm 0.5\ min^{-1}$, $K = 39 \pm 6$ mM).

Steady-state kinetic data, obtained in studies with sarcosine at 25 °C, exhibit the following features: (i) Double-reciprocal plots of reaction rate versus sarcosine concentration intersect on the *y*-axis, as judged by linear regression analysis of data obtained at each oxygen concentration tested; (ii) double-reciprocal plots of reaction rate versus oxygen concentration intersect to the left of the *y*-axis and above the *x*-axis. (iii) Secondary plots of slopes and intercepts are linear. The secondary plot of slopes versus 1/[sarcosine] passes through the origin. These features are consistent with a rapid equilibrium ordered mechanism with oxygen as the first substrate to bind (Scheme 2). Figure 5 shows the global fit of the data to an equation for a rapid equilibrium ordered mechanism (eq 6). The global fit yielded values for steady-state kinetic parameters similar to those estimated by linear regression analysis (Table 2). The observed turnover rate at 25 °C (24.5 min^{-1}) is 3.6-fold faster than the limiting rate

Scheme 2: Rapid Equilibrium Ordered Mechanism

$$E_{ox} \underset{k_{-1}}{\overset{k_1[O_2]}{\rightleftharpoons}} E_{ox}{\cdot}O_2 \underset{k_{-2}}{\overset{k_2[S]}{\rightleftharpoons}} E_{ox}{\cdot}S{\cdot}O_2 \underset{k_{-3}}{\overset{k_3}{\rightleftharpoons}} E_{red}{\cdot}P{\cdot}O_2 \underset{k_{-4}}{\overset{k_4}{\rightleftharpoons}} E_{ox}{\cdot}P{\cdot}Q \underset{k_{-5}}{\overset{k_5}{\rightleftharpoons}} E_{ox}$$

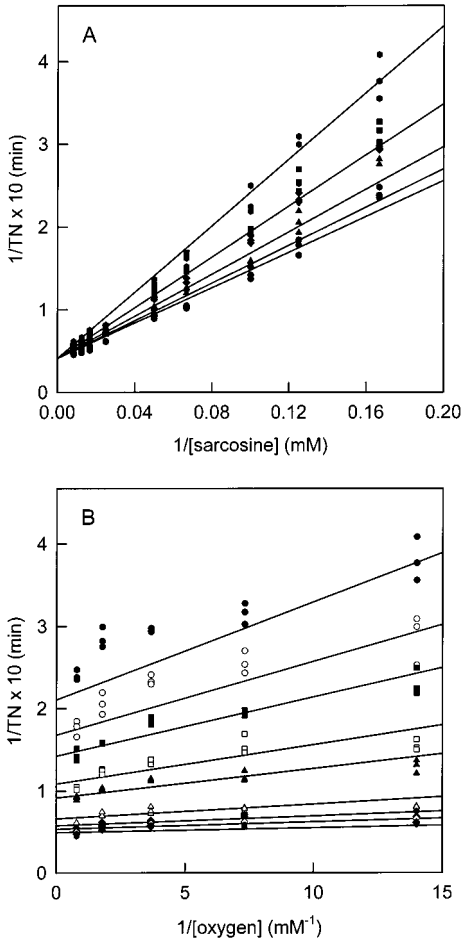

FIGURE 5: Steady-state kinetic data for MTOX with sarcosine as substrate. Measurements were made at 25 °C in 100 mM potassium phosphate buffer, pH 8.0. Panel A shows double reciprocal plots at various oxygen concentrations [1.27 mM (filled circles), 0.56 mM (filled triangles), 0.27 mM (filled diamonds), 0.14 mM (filled squares), and 0.072 mM (filled hexagons)]. Panel B shows double reciprocal plots at various sarcosine concentrations [120 mM (filled hexagons), 80 mM (open diamonds), 60 mM (filled diamonds), 40 mM (open triangles), 20 mM (filled triangles), 15 mM (open squares), 10 mM (filled squares), 8 mM (open circles), 6 mM (filled circles). The lines show the fit of the data to eq 6.

Table 2: Comparison of Steady State and Reductive Half-Reaction Kinetic Parameters with Sarcosine as Substrate[a]

parameter	steady state	half-reaction
k_{cat} (min^{-1})	24.5 ± 0.7 (28.3)	
k_{lim} (min^{-1})		6.8 ± 0.5
$K_{sarcosine}$ (mM)	25 ± 2 (35)	39 ± 6
K_{oxygen} (mM)	0.072 ± 0.01 (0.045)	

[a] Steady-state kinetic parameters were determined at 25 °C by fitting the data to an equation for a rapid equilibrium ordered mechanism (eq 6). The values shown in parentheses were determined by linear regression analysis of double reciprocal plots, as described in the text. Reductive half-reaction kinetic parameters were determined at 4 °C by fitting the data to eq 1.

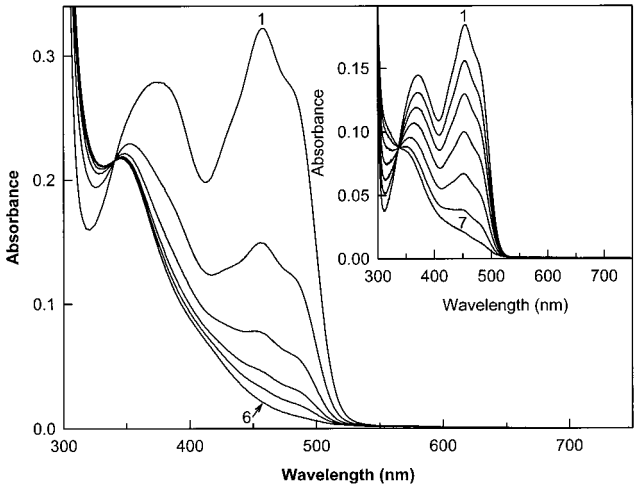

FIGURE 6: Anaerobic reaction of MTOX with formaldehyde and L-tryptophan. A small aliquot of MTOX was tipped from the sidearm of an anaerobic cuvette into a reaction mixture containing 1 mM formaldehyde, 1 mM L-tryptophan, and 1 mM EDTA in 50 mM potassium phosphate buffer, pH 8.0, at 25 °C. Curves 1−6 were recorded 0.33, 2.5, 5, 7.5, 10, and 40 min, respectively, after mixing. The inset shows the reaction with MSOX, conducted under the same conditions except that the buffer did not contain EDTA and 1 mM glycine replaced L-tryptophan. Curves 1−7 were recorded 0.4, 10.4, 20.4, 35.4, 60.4, 105.4, and 245.4 min, respectively, after mixing.

of the anaerobic half-reaction at 4 °C (6.8 min^{-1}), a difference attributed to the 21 °C temperature difference between the two sets of measurements.

Anaerobic Reaction of MTOX with Formaldehyde and L*-Tryptophan.* Double reciprocal plots in a modified ping pong mechanism can appear almost parallel, as observed with *N*-methyl-L-tryptophan, if the reductive half-reaction is irreversible (e.g., Scheme 1, $k_{-2} \sim 0$). We hoped to evaluate the reversibility of the reductive half-reaction of MTOX with *N*-methyl-L-tryptophan by determining whether *N*-methyl-L-tryptophan imine (formed in situ by mixing formaldehyde with L-tryptophan) could reoxidize 2-electron reduced MTOX [$EFADH_2$, generated by photoreduction (*3*)]. However, a surprising result obtained in a control reaction showed that the planned reversibility experiment would not be feasible. In the control reaction, *oxidized* MTOX was mixed with 1 mM formaldehyde and 1 mM L-tryptophan under anaerobic conditions. An isosbestic conversion to 1,5-dihydroFAD was observed in an apparent first-order reaction ($k_{obs} = 0.369 \pm 0.003$ min^{-1}) that was fully reversible upon aeration (Figure 6). No reaction was observed upon mixing MTOX with formaldehyde or L-tryptophan alone. A similar reduction reaction was observed with MSOX upon reaction with 1 mM formaldehyde and 1 mM glycine (Figure 6, inset) except that the MSOX reaction was more than an order of magnitude slower ($k_{obs} = 0.0206 \pm 0.0001$ min^{-1}).

The carbinolamine formed in amino acid/formaldehyde mixtures would appear to be the most likely reductant of MTOX (or MSOX) since it resembles the corresponding *N*-methyl amino acid substrate except that one of the hydrogens on the *N*-methyl group is replaced by a hydroxyl.

Scheme 3: Oxidation of the Carbinolamine, Present in Amino Acid/Formaldehyde Mixtures, to the Corresponding N-Formyl Amino Acid by MTOX and MSOX

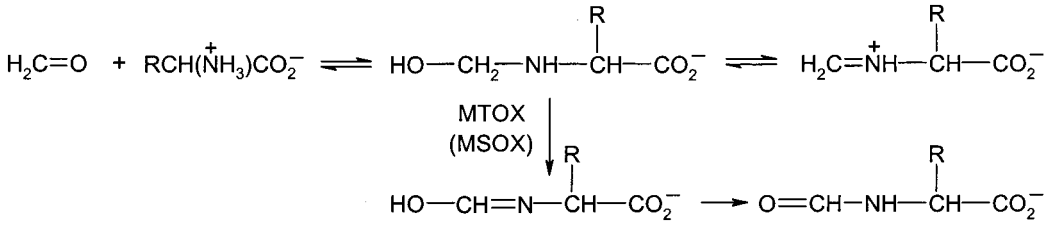

Oxidation of the C−N bond in the carbinolamine, followed by tautomerization, would generate the corresponding *N*-formyl amino acid (Scheme 3). To test this hypothesis, an aerobic reaction mixture containing MTOX (17.3 μM), 1 mM formaldehyde, 1 mM L-tryptophan, and 1 mM EDTA in 5 mM potassium phosphate buffer, pH 8.0, was incubated at room temperature with shaking. After 5.3 h, the sample was microfiltered to remove protein. Quantitative conversion of L-tryptophan to *N*-formyl-L-tryptophan was observed when the filtrate was analyzed by thin-layer chromatography (solvent A), as detailed in Experimental Procedures. No *N*-formyl-L-tryptophan was found in a control incubation without MTOX.

In a separate experiment, MTOX (3.1 μM) was incubated with 1 mM *N*-methyl-L-tryptophan in place of L-tryptophan and formaldehyde. The oxidative demethylation of *N*-methyl-L-tryptophan to L-tryptophan was complete within 15 min under these conditions, as judged by thin-layer chromatography (solvent B). Formation of *N*-formyl-L-tryptophan was not detectable after 15 min but was observed over a period of hours, accompanied by the disappearance of L-tryptophan. The results indicate that the product(s) formed upon 2-electron oxidation of *N*-methyl-L-tryptophan are released into solution. Further oxidation to N-formyl-L-tryptophan occurs in a secondary, slower reaction that is not competitive with *N*-methyl-L-tryptophan oxidation.

N-Formyl-DL-tryptophan forms a spectrally detectable complex with MTOX. The complex exhibits a difference spectrum similar to that observed with glycine derivatives (*N*,*N*′-dimethylglycine, *N*-benzylglycine), except for a bathochromic shift of the negative peak around 350 nm. The spectral perturbation observed with these N-substituted amino acids appears to be nearly a mirror image of that observed with aromatic carboxylates, such as benzoate (*3*) (Figure 7). The stability of the MTOX•*N*-formyltryptophan complex (K_d = 1.28 ± 0.05 mM, not corrected for the presence of the D-isomer) is within the range observed for the best known MTOX ligands (e.g., 3-indolepropionate, K_d = 0.79 mM) (*3*).

Reduction of MTOX with Thioglycolate. Thioglycolate causes a small spectral perturbation upon binding to MTOX under aerobic conditions (data not shown), forming a complex of modest stability (K_d = 120 ± 20 mM) with no evidence of charge transfer interaction. However, under anaerobic conditions this complex is observed to undergo two successive, 1-electron transfer reactions that result in the conversion of oxidized enzyme to 1,5-dihydroFAD. The reaction proceeds via the nearly quantitative formation of a red, anionic flavin radical intermediate (Figure 8, panel A), as judged by the development of an intense new absorption band at 393 nm similar to that observed for the radical formation via 5-deazariboflavin-mediated photoreduction (*3*). The radical is converted to 1,5-dihydroFAD in the second, slower phase of the reaction (Figure 8, panel B). The spectral changes at 450 and 393 nm gave a good fit to a two-exponential expression (eq 3) (Figure 8, insets). The same rate constants are obtained upon analysis at either wavelength. The observed rate of radical formation (k_{obs} = 1.2 × 10^{-2} min^{-1}) is about an order of magnitude faster than radical reduction to 1,5-dihydroFAD (k_{obs} = 1.4 × 10^{-3} min^{-1}).

DISCUSSION

Turnover of MTOX with *N*-methyl-L-tryptophan appears to proceed via a modified ping pong mechanism where oxygen binds to the reduced enzyme prior to dissociation of imino acid product (Scheme 1). Although double reciprocal plots with *N*-methyl-L-tryptophan as the varied substrate are nearly parallel, the slopes show a small but systematic variation depending on the oxygen concentration. *N*-benzylglycine, a dead-end competitive inhibitor with respect to *N*-methyl-L-tryptophan, acts as a noncompetitive inhibitor with respect to oxygen, a result that provides further evidence for a modified, rather than a classic, ping pong mechanism. Although *N*-methyl-L-tryptophan is the best known substrate for MTOX, the enzyme will also catalyze the oxidation of other *N*-methyl amino acids, including sarcosine which is a poor substrate exhibiting a turnover rate about 0.5% of that observed with *N*-methyl-L-tryptophan. *N*,*N*′-Dimethylglycine forms a complex with MTOX but is not oxidized (*3*), suggesting that MTOX is specific for secondary amines. We have identified carbinolamines as a new class of alternate substrate for MTOX. Oxidation of the carbinolamine, formed in L-tryptophan/formaldehyde mixtures, yields *N*-formyl-L-tryptophan (Scheme 3). The reaction is relatively slow and does not compete with turnover of the enzyme with *N*-methyl-L-tryptophan.

In a modified ping pong mechanism (Scheme 1), double reciprocal plots will appear nearly parallel if the $K_{ia}K_b$ term in eq 4 is small, a condition that can arise when $k_{-1} \approx 0$ (sticky substrate) or $k_{-2} \approx 0$ (reductive step is irreversible). It was not possible to evaluate the reversibility of the reductive step with *N*-methyl-L-tryptophan by determining whether reduced enzyme could be reoxidized by *N*-methyl-L-tryptophan imine because formaldehyde/L-tryptophan mixtures (required for in situ imine formation) would also contain the corresponding carbinolamine, a known reductant of oxidized MTOX. Evidence regarding the reversibility of the reductive step was obtained in reductive half-reaction kinetic studies using sarcosine as substrate. The reductive half-reaction with sarcosine at 4 °C exhibited saturation kinetics (k_{lim} = 6.8 min^{-1}, K = 39 mM). A double reciprocal plot of the data was linear with a finite *y*-intercept. The results are

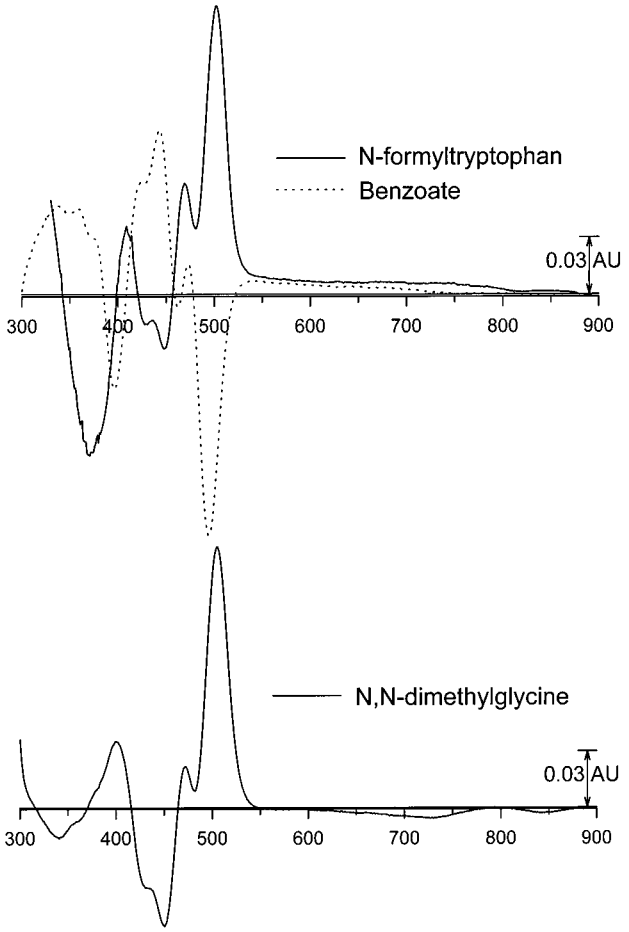

FIGURE 7: Comparison of the difference spectrum observed for the MTOX complex with *N*-formyl-DL-tryptophan with difference spectra reported (*3*) for MTOX complexes with benzoate and *N*,*N*′-dimethylglycine. Spectra are normalized as described in Experimental Procedures.

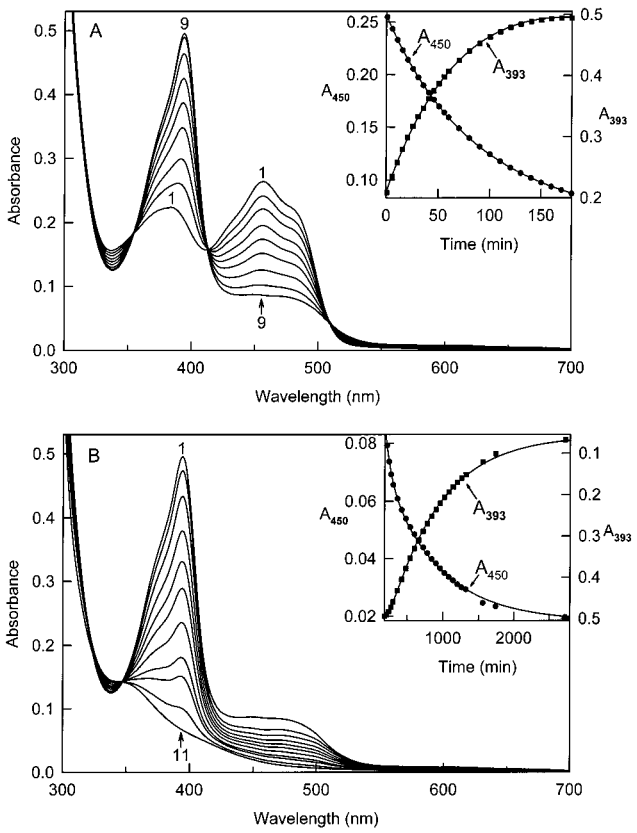

FIGURE 8: Anaerobic reaction of MTOX with thioglycolate. Panel A shows the first phase of the reaction. Curves 1−9 were recorded 0.75, 10.75, 20.75, 35.75, 50.75, 70, 100, 140, and 180 min, respectively, after mixing MTOX with 0.3 M thioglycolate in 50 mM potassium phosphate buffer, pH 8.0, containing 1 mM EDTA at 25 °C. Panel B shows the second phase of the reaction. Curves 1−11 were recorded 3, 4.5, 6, 8, 10, 12, 15, 19, 22, 29, and 45.5 h, respectively, after mixing. Absorbance changes at 450 and 393 nm over the entire reaction course were fitted to a two-exponential expression (eq 3). The solid lines in the insets to panels A and B show the fit results for the first and second phases of the reaction, respectively. The scale of the *y*-axis for A_{393} in the inset to panel B has been reversed for clarity in data presentation.

consistent with a reductive half-reaction where $k_{-2} \approx 0$ and $k_{-1} \gg k_2$, as judged by criteria described by Strickland et al. (*15*). This means that a nearly irreversible reduction step is preceded by a rapidly attained equilibrium between free E and the E·S complex. Under these conditions k_{lim} is the rate of the reductive step (k_2) and K is the dissociation constant for the E·S complex. Significantly, the K_d value estimated for MTOX•sarcosine complex is comparable to the K_d determined by spectral titration for the structurally similar complex formed with MTOX and dimethylglycine (K_d = 32.4 mM, 4 °C) (*3*).

The 3.6-fold lower value estimated for the limiting rate of the reductive half-reaction with sarcosine at 4 °C, as compared with aerobic turnover at 25 °C (6.8 versus 24.5 min^{-1}) is reasonably attributable to the 21 °C temperature difference in the two sets of experiments. The results, therefore, indicate that sarcosine is oxidized at a kinetically significant rate under anaerobic conditions and suggest that the reductive half-reaction is rate-limiting during turnover under aerobic conditions. These conclusions appear, however, difficult to reconcile with the steady-state kinetic patterns observed with sarcosine that are consistent with a rapid equilibrium ordered mechanism with oxygen as the *first* substrate (Scheme 2). The data might be reconciled by assuming a random mechanism with strong synergism in the binding of oxygen and sarcosine, analogous to that proposed for glycerokinase where an equilibrium ordered mechanism was observed with amino analogues of glycerol (MgATP binds first) versus an ordered mechanism with glycerol (MgATP binds second) (*16*). In this scenario, oxygen might appear to bind first if (i) The K_d for the MTOX•oxygen complex is much less than the MTOX•sarcosine complex; *and* (ii) The presence of oxygen leads to much tighter binding of sarcosine. The first criterion is reasonably satisfied, as judged by comparison of the K_d values estimated for the MTOX•oxygen (72 μM) and MTOX•sarcosine (39 mM) complexes by analysis of steady state and reductive half-reaction kinetic data, respectively. The second criterion does not, however, appear to be satisfied since the K_d estimated for sarcosine dissociation from the MTOX•oxygen•sarcosine complex from steady-state data (25 mM), is very similar to the value estimated for the MTOX•sarcosine complex (39 mM). [The temperature difference in the two experiments (25 °C versus 4 °C) is probably not critical, as judged by the similar binding observed for *N*,*N*′-dimethylglycine at the two temperatures (K_d = 49.9 versus 32.4 mM, respectively; *3*)]. In the absence of a metal center, it is difficult to envision the basis for the apparent stability of the MTOX•oxygen complex. To the best of our knowledge, there is no precedent

Scheme 4: Possible Mechanisms for Substrate Oxidation by MTOX[a]

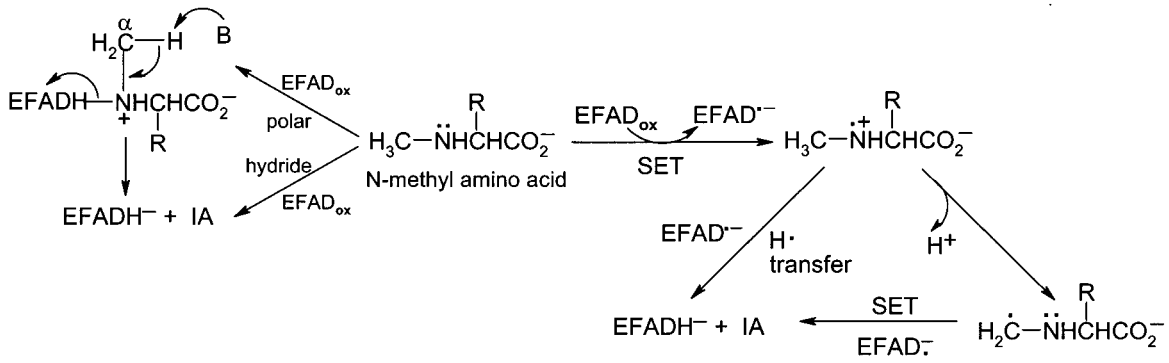

[a] IA = imino acid.

for the formation of a E•oxygen complex with the oxidized form of any other flavoenzyme.

The detailed mechanism of amine to imine oxidation by flavoenzymes has received considerable attention but is still quite controversial. Studies with mechanism-based inactivators of monoamine oxidase (*17*, *18*) and, more recently, MSOX (*19*) are consistent with amine oxidation by one of two variants of a single electron transfer (SET) mechanism. The two variants both involve initial 1-electron transfer from substrate amino group, generating a flavin radical intermediate, but differ with respect to the mechanism of the second oxidation step (H• versus H^+ plus $1e^{-1}$) (Scheme 4). A hydride transfer mechanism has been proposed for D-amino acid oxidase (*20*). Amine oxidation via a polar mechanism, involving formation of a covalent flavin-substrate intermediate (4a-flavin adduct), has been observed in flavin model studies (*21*, *22*) (Scheme 4). No evidence for the formation of a flavin radical or 4a-adduct intermediate was obtained by monitoring the spectral course of the anaerobic reduction of MTOX by sarcosine or the carbinolamine formed with L-tryptophan and formaldehyde. In the case of a SET mechanism, a detectable flavin radical is not expected since the intermediate would be generated in a thermodynamically unfavorable step [$E° = +0.7$ to 1 V for the $RNH_2^{•+}/RNH_2$ couple with aliphatic amines) (*23*)] and should rapidly be converted to 1,5-dihydroFAD.

We reasoned that thioglycolate ($HSCH_2CO_2^-$) might form a detectable 4a-adduct with MTOX since (i) Thiols are known to form 4a-flavin adducts (*24*), analogous to the putative 4a-flavin-substrate intermediate; (ii) The 4a-thioglycolate adduct could not undergo further reaction to yield the 2-electron reduced flavin, unlike the 4a-flavin-substrate adduct; and (iii) The sulfur in an initial noncovalent MTOX•thioglycolate complex should be properly positioned for nucleophilic attack at flavin C4(a), assuming a binding mode similar to that observed for the related MSOX complex with methylthioacetate ($CH_3SCH_2CO_2^-$) (*9*, *10*). MTOX was found to bind thioglycolate, forming a noncovalent complex. Under anaerobic conditions, this complex was observed to undergo two successive, 1-electron transfer steps, generating 1,5-dihydroFAD in a reaction that proceeded via a red, anionic flavin radical intermediate. Flavin radical formation should be thermodynamically unfavorable, based on $E°$ values reported for the $RS^•/RS^-$ or $RS^{•+}H/RSH$ couple ($E° = +0.78$ or $+1.35$ V, respectively) (*25*) as compared with those observed for the $EFl/EFl^{•-}$ or $EFl/EFlH^•$ couple with other flavoenzymes ($E° = -0.3$ to $+0.3$ V) (*26*, *27*). The observed nearly quantitative radical formation suggests that back electron transfer is prevented by dissociation of the thiolate radical, followed by the binding of a molecule of unreacted thioglycolate (present in excess) to form a relatively stable $EFAD^{•-}$•thioglycolate complex where radical reduction occurs at a rate that is about an order of magnitude slower than radical formation. An analogous 1-electron-transfer reaction is observed with MSOX and thioglycolate but radical formation is slower and further reduction to 1,5-dihydroFAD is not observed (*11*).

ACKNOWLEDGMENT

We thank Drs. John Schloss and W. Wallace Cleland for helpful advice and useful discussions. We acknowledge Dr. Mary Ann Wagner for the initial finding that MSOX is reduced in the presence of glycine and formaldehyde. We thank Dr. Gouhua Zhao for his generous gift of purified MSOX.

REFERENCES

1. Wagner, M. A., Khanna, P., and Jorns, M. S. (1999) *Biochemistry 38*, 5588−5595.
2. Koyama, Y., and Ohmori, H. (1996) *Gene 181*, 179−183.
3. Khanna, P., and Jorns, M. S. (2001) *Biochemistry 40*, 1441−1450.
4. Kvalnes-Krick, K., and Jorns, M. S. (1991) in *Chemistry and Biochemistry of Flavoenzymes* (Muller, F., Ed.) pp 425−435, CRC Press, Inc., Boca Raton.
5. Cannon, J. R., and Williams, J. R. (1982) *Aust. J. Chem. 35*, 1497−1500.
6. Jansen, R., Kunze, B., Reichenbach, H., and Hoefle, G. (1996) *Liebigs Ann. Org. Bioorg. Chem. 2*, 285−290.
7. Chlumsky, L. J., Zhang, L., and Jorns, M. S. (1995) *J. Biol. Chem. 270*, 18252−18259.
8. Reuber, B. E., Karl, C., Reimann, S. A., Mihalik, S. J., and Dodt, G. (1997) *J. Biol. Chem. 272*, 6766−6776.
9. Trickey, P., Wagner, M. A., Jorns, M. S., and Mathews, F. S. (1999) *Structure 7*, 331−345.
10. Wagner, M. A., Trickey, P., Chen, Z., Mathews, F. S., and Jorns, M. S. (2000) *Biochemistry 39*, 8813−8824.
11. Wagner, M. A., and Jorns, M. S. (2000) *Biochemistry 39*, 8825−8829.
12. Ahmed, S. A., and Claiborne, A. (1992) *J. Biol. Chem. 267*, 25822−25829.
13. Fersht, A. (1977) *Enzyme Structure and Mechanism*, pp 134−155, W. H. Freeman and Company, Reading.
14. Fromm, H. J. (1979) *Methods Enzymol. 63*, 467−486.
15. Strickland, S., Palmer, G., and Massey, V. (1975) *J. Biol. Chem. 250*, 4048−4052.

16. Knight, W. B., and Cleland, W. W. (1989) *Biochemistry 28*, 5728−5734.
17. Silverman, R. B. (1995) *Acc. Chem. Res. 28*, 335−342.
18. Silverman, R. B., and Zelechonok, Y. (1992) *J. Org. Chem. 57*, 6373−6374.
19. Zhao, G., Qu, J., Davis, F. A., and Jorns, M. S. (2000) *Biochemistry 39*, 14341−14347.
20. Mattevi, A., Vanoni, M. A., Todone, F., Rizzi, M., Teplyakov, A., Coda, A., Bolognesi, M., and Curti, B. (1996) *Proc. Natl. Acad. Sci. U.S.A. 93*, 7496−7501.
21. Kim, J. M., Bogdan, M. A., and Mariano, P. S. (1993) *J. Am. Chem. Soc. 115*, 10591−10595.
22. Kim, J. M., Hoegy, S. E., and Mariano, P. S. (1995) *J. Am. Chem. Soc. 117*, 100−105.
23. Chow, Y. L., Danen, W. C., Nelsen, S. F., and Rosenblatt, D. H. (1978) *Chem. Rev. 78*, 243−278.
24. Yokoe, I., and Bruice, T. C. (1975) *J. Am. Chem. Soc. 97*, 450−451.
25. Armstrong, D. A. (1999) in *S-Centered Radicals* (Alfassi, Z. B., Ed.) pp 27−61, John Wiley and Sons, New York.
26. Stankovich, M. T. (1991) in *Chemistry and Biochemistry of Flavoenzymes* (Muller, F., Ed.) pp 401−425, CRC Press, Boca Raton, FL.
27. Ramsay, R. R., Sablin, S. O., and Singer, T. P. (1995) *Prog. Brain Res. 106*, 33−39.

BI002442T